

Numerical Heat Transfer, Part B: Fundamentals

An International Journal of Computation and Methodology

ISSN: (Print) (Online) Journal homepage: www.tandfonline.com/journals/unhb20

Entropy production in the flow of Bingham-Papanastasiou fluid having temperature and shear rate-dependent viscosity

Muhammad Idrees Afridi, Zafar Ali, Muhammad Qasim & Ali J. Chamkha

To cite this article: Muhammad Idrees Afridi, Zafar Ali, Muhammad Qasim & Ali J. Chamkha (15 Apr 2024): Entropy production in the flow of Bingham-Papanastasiou fluid having temperature and shear rate-dependent viscosity, Numerical Heat Transfer, Part B: Fundamentals, DOI: [10.1080/10407790.2024.2341093](https://doi.org/10.1080/10407790.2024.2341093)

To link to this article: <https://doi.org/10.1080/10407790.2024.2341093>



Published online: 15 Apr 2024.



Submit your article to this journal [↗](#)



Article views: 35




View related articles [↗](#)



View Crossmark data [↗](#)



Entropy production in the flow of Bingham-Papanastasiou fluid having temperature and shear rate-dependent viscosity

Muhammad Idrees Afridi^a , Zafar Ali^b, Muhammad Qasim^b, and Ali J. Chamkha^c 

^aSchool of Mathematics and Computer Science, Hanjiang Normal University, Shiyao, China; ^bDepartment of Mathematics, COMSATS University Islamabad (CUI), Pakistan; ^cFaculty of Engineering, Kuwait College of Science and Technology, Doha District

ABSTRACT

This article comprehensively examines entropy production in a peristaltic flow of Bingham-Papanastasiou fluid in an asymmetric wavy wall channel. The viscosity of the fluid is selected to depend on the temperature in addition to the shear rate. Furthermore, viscous dissipation is considered. The equations governing momentum and energy are adjusted to incorporate the existence of a nonlinear correlation between stress and strain rate. The energy dissipation caused by viscosity in the energy equation exhibits variation between Newtonian and non-Newtonian fluids due to their distinct rheological behaviors and response to shear forces. Newton's law of viscosity states that the viscous dissipation term for Newtonian fluids follows a simple linear relationship between shear stress and shear rate. In contrast, non-Newtonian fluids exhibit more complex rheological behaviors, with the correlation between shear stress and shear rate described by various constitutive equations, depending on the specific type of non-Newtonian behavior. Consequently, the energy equation for non-Newtonian fluid flow problems becomes more intricate and nonlinear compared to the energy equation for Newtonian fluids, resulting in a more challenging analysis. Modeling of the equations is traditionally obtained using all steps involved in analyzing peristaltic flow. Using MATLAB's `bvp5c` solver, the obtained coupled set of differential equations is numerically solved. The research explores how the Bingham number and stress growth exponent parameters affect different dimensionless variables, including velocity, streamlines, temperature, axial pressure gradient, entropy production, and the Bejan number.

ARTICLE HISTORY

Received 19 December 2023
Revised 1 April 2024
Accepted 4 April 2024

KEYWORDS

Bejan number; Bingham-Papanastasiou fluid; entropy generation minimization; heat transfer; temperature-dependent viscosity; wavy wall channel

1. Introduction

Peristaltic flows entail fluid transfer in a tube or channel through sequential wall contractions and relaxations within the conduit. It is a fundamental mechanism for moving substances within the human body and other living organisms. In physiology, peristaltic flow is observed in several biological systems, including capillaries, the gastrointestinal tract, the ureter, the bile duct, the esophagus, and the reproductive tracts. This rhythmic and coordinated motion plays a fundamental role in propelling fluids and substances through these anatomical structures, ensuring the transport and functionality of vital physiological processes. It is not limited to biological systems; peristaltic flow can also be used in various industrial and engineering applications, such as transporting fluids with precision and controlled through blood pumps for dialysis, roller pumps,

Nomenclature

A_1, A_2	Amplitudes of upper and lower waves	Re	Reynolds number
Be	Bejan number	T	Dimensional temperature fields
Br	Brinkman number	\bar{U}, \bar{V}	Dimensional velocity components in laboratory frame
B_n	Bingham number	\bar{u}, \bar{v}	Dimensional velocity components in wave frame
c	Wave speed	\bar{X}, \bar{Y}	Space coordinates in laboratory frame
C_p	Specific heat	\bar{x}, \bar{y}	Space coordinates in wave frame
\dot{E}_{gen}	Volumetric Entropy generation rate	α	Variable viscosity parameter
$(\dot{E}_{gen})_0$	Characteristic entropy	γ	Variable thermal conductivity parameter
F	Dimensionless flow rate in wave frame.	μ	Dynamic viscosity
G^*	Stress growth parameter	ρ	Density of fluid
\bar{H}_1, \bar{H}_2	Upper and lower walls	λ	Wavelength
k	Thermal conductivity	ϕ	Phase difference
Ns	Entropy generation number	ψ	Dimensionless stream function
\bar{P}, \bar{p}	Pressure fields in laboratory and wave frame		
\bar{Q}, q	Dimensional flow rate in laboratory and wave frame		

finger pumps, and in the transportation of corrosive fluids which necessitates the prevention of direct contact between the fluid and machinery components. Latham [1] was the pioneer researcher to study fluid movement through peristaltic pumping and opened a new research door to study fluid flows. After Latham's seminal research, numerous scientists and engineers have significantly contributed to understanding and applying peristaltic flows in various fields, particularly physiology, biological systems, and engineering.

Non-Newtonian fluids, including substances like oils, paints, lubricants, drilling muds, molten plastics and polymers, gels, rubber solutions, and various biological fluids, exhibit behaviors that deviate from the classical laws of fluid viscosity, commonly referred to as Newton's law of viscosity. When it comes to non-Newtonian fluids the nonlinear correlation between shearing stress and shear rate adds a level of complexity that is now crucial to understanding these fluids in modern scientific and technical fields. The significance of understanding non-Newtonian fluids has grown considerably, particularly in the realms of modern chemical engineering, lubrication technology, soil mechanics, biophysics, and related fields. This is due to the wide-ranging applications and implications of these fluids in various industrial and biological processes. Multiple factors contribute to the departure of these fluids from Newtonian characteristics. Two key factors include structural changes occurring within the fluid as it experiences shear forces and the dependence of the stress tensor on the immediate deformation state. The fact that this dependence is essentially nonlinear and can be described as a function of the strain tensor's rate highlights the complexity of these fluids. This nonlinearity in the behavior of non-Newtonian fluids has led to the establishment of various classifications to describe their diverse responses to different conditions and forces. Therefore, no constitutive equation can accurately predict the behavior of all non-Newtonian fluids. In recognition of this complexity, rheologists, experts in the study of the flow and deformation of matter, have proposed a multitude of constitutive equations [2–5] to provide a framework for comprehending and characterizing the features of non-Newtonian fluids across different scenarios and applications. Studies [6–14] have reported the peristaltic flows of different non-Newtonian fluids. One of the groups of non-Newtonian fluids called viscoplastic materials possesses a yield stress limit which on exceeding the threshold makes deformation in the fluids. Linear Bingham [15], nonlinear Herschel-Bulkley [16], and the Casson models [17] relations are proposed to define stress-strain relations in such fluids. Viscoplastic fluids lack deformations when the force applied is less than the set threshold. Bingham fluid is also the case

of a viscoplastic fluid named after Bingham [18]. In industrial processes, Bingham fluid modeling is important since many materials show viscoplastic characteristics [19]. Yet, the model of the Bingham fluid is not capable of being studied and exploited in complex situations because of fact that some part of the fluid flows while other remains solid. This created difficulties in locating and understanding the shape of yield surfaces because two different constitutive equations were used across them. Also, the apparent viscosity of Bingham model becomes infinite on vanishing the shear rates, this creates discontinuity in the equations and numerical difficulties. Papanastasiou [20] overcame the issue by introducing the modified Bingham fluid model. Thus, the rheological behavior of the Bingham fluid is approximated by Bingham-Papanastasiou fluid model [21–24]. Soto *et al.* [25] numerically investigated the yield stress of Bingham-Papanastasiou fluid through sudden planar expansion. Daniel *et al.* [26] chose Bingham-Papanastasiou regularization as a source to explain the nonlinear yield stress and the shear-dependent viscosity of Magneto-Rheological Fluids. Khan and Sultan [27] numerically studied the flow of Bingham-Papanastasiou fluid generated by infinite rotating disk. Modeling the peristaltic flow of Bingham-Papanastasiou fluid is of prime interest because of the fact that such flows are suitable for highly viscous fluids like; sterile fluids, waxy oils, foams, and solids slurries [28,29]. Physiological fluids like blood, mucus, etc. behave like Bingham-Papanastasiou fluid that is transported by peristaltic motion. Tripathi and Beg [30] theoretically investigated the peristaltic flow of rheological viscoplastic fluids inside the physiological ducts. The electro-osmotically enhanced peristaltic motion of Bingham-Papanastasiou fluid in an asymmetric channel was reported by Aslam and Noreen [31].

In heat transfer and fluid flow problems, the second law of thermodynamics is used to measure the irreversibility of the systems, called entropy. It is the measure of disorder in the system due to an irreversible process. Analysis of entropy generation is used to explain and locate the sources that decay the energy of the system and find ways to obtain optimal energy by diminishing such sources. The concept of entropy was pioneered by Bejan [32], in which he studied four configurations of the convective heat transfer phenomenon. Entropy generation minimization was also proposed by Bejan [33] in the pursuit of optimizing thermal designs and efficiency of thermodynamical systems. Here, Bejan [33] disclosed that heat transfer and viscous dissipation arising from the fluid's viscous effects are the two primary sources of entropy creation in thermal systems. Thereafter, many researchers around the globe have been engaged and encouraged to study the entropy generation in Newtonian and non-Newtonian fluids due to its essential applications. Makinde and Eegunjobi [34] explored the entropy generation of Magneto-hydrodynamic MHD Newtonian fluids in porous media. Shit and Mondal [35] explored the entropy generation of non-Newtonian fluid by considering the impacts of radiation. The entropy generation of a three-dimensional flow of a dissipative hybrid nanofluid was examined by Afridi *et al.* [36]. Qasim *et al.* [37] conducted a study to examine the entropy generation in a flow around a slender radiative needle moving within a parallel stream. Qasim *et al.* [38] again explored the entropy generation in nanofluids inside a sinusoidal wavy channel. A considerable amount of work on entropy generation of peristaltic flows is done for Newtonian and non-Newtonian fluids as because of its importance in biomedical systems. Entropy generation of MHD fluids with joule heating is analyzed by Ranjit and Shit [39] in an electro-osmotic and peristaltic flow. Akbar and Butt [40] performed the analysis of nanofluids flowing peristaltically in a tube with viscous dissipation. Hayat *et al.* [41] studied the irreversibility analysis of nanomaterial in a rotating frame. Saleem [42] studied entropy of peristaltic flows in asymmetric channel using space-dependent viscosity. Narla *et al.* [43] observed entropy production of MHD fluids in curved channels taking Ohmic heating in action.

Several materials' transport properties (viscosity, electric, and thermal conductivity) vary significantly with temperature. The researchers examine peristaltic flows with variable transport properties [44–48]. The entropy formation during peristaltic flow with varying fluid properties

was scrutinized by Qasim *et al.* [49]. A review of relevant literature witnessed that no research has been conducted on the peristaltic flow of Bingham-Papanastasiou fluid in an asymmetric channel. Therefore, the present research is being performed to explore the entropy production in this flow by considering variable thermal conductivity and viscosity. In this study, the resulting equations are coupled and nonlinear, so to find the approximate solution of this nonlinear system, a numerical solution is computed using bvp5c MATLAB [50,51]. The impact of physical parameters, namely, the Bingham number (B_n) and the stress growth exponent parameter (G) on different dimensionless quantities, including entropy generation number, velocity, axial pressure gradient, temperature, streamlines, and Bejan number are examined.

2. Problem statement

We considered the peristaltic flow of the Bingham-Papanastasiou fluid in an asymmetric channel whose walls have the mathematical expressions defined below.

$$\begin{aligned}\bar{Y} &= \bar{H}_1(\bar{X}, \bar{t}) = L_1 + A_1 \cos \left[\frac{2\pi}{\lambda} (\bar{X} - c\bar{t}) \right], \\ \bar{Y} &= \bar{H}_2(\bar{X}, \bar{t}) = -L_2 - A_2 \cos \left[\frac{2\pi}{\lambda} (\bar{X} - c\bar{t}) + \phi \right].\end{aligned}\quad (1)$$

where $\bar{H}_2(\bar{X}, \bar{t})$ is the lower whereas $\bar{H}_1(\bar{X}, \bar{t})$ is the upper wall. The rectangular coordinates \bar{X} and \bar{Y} are taken along the channel length and normal to the walls of the channel, respectively and the time coordinate is denoted by \bar{t} . c is the wave speed, A_1 and A_2 are the amplitudes of the upper and lower waves, λ is the wavelength, and $\phi \in [0, \pi]$ is the phase difference. The Cauchy stress tensor of this model by considering temperature-dependent viscosity is expressed in the following form [20–24]:

$$\bar{\Gamma}_{ij} = \left[\bar{\mu}(\bar{T}) + \frac{\tau_y}{|\bar{\gamma}|} (1 - e^{-G^*|\bar{\gamma}|}) \right] \bar{\gamma}_{ij}. \quad (2)$$

where $\bar{\gamma}_{ij}$ is defined as

$$\bar{\gamma}_{ij} = \left(\frac{\partial u_i}{\partial x_j} + \frac{\partial u_j}{\partial x_i} \right). \quad (3)$$

In Eq. (2), where G^* is the stress growth parameter, τ_y denotes the yield stress, and $|\bar{\gamma}|$ is the second invariant of the rate of strain tensor expressed by

$$|\bar{\gamma}| = \sqrt{\frac{1}{2} \bar{\gamma}_{ij} \bar{\gamma}_{ij}}. \quad (4)$$

The component form of the governing equations (continuity, momentum, and energy) in a fixed frame are

$$\frac{\partial \bar{U}}{\partial \bar{X}} + \frac{\partial \bar{V}}{\partial \bar{Y}} = 0, \quad (5)$$

$$\rho \left(\frac{\partial}{\partial \bar{t}} + \bar{U} \frac{\partial}{\partial \bar{X}} + \bar{V} \frac{\partial}{\partial \bar{Y}} \right) \bar{U} = -\frac{\partial \bar{P}}{\partial \bar{X}} + \frac{\partial}{\partial \bar{X}} (\Gamma_{\bar{X}\bar{X}}) + \frac{\partial}{\partial \bar{Y}} (\Gamma_{\bar{X}\bar{Y}}), \quad (6)$$

$$\rho \left(\frac{\partial}{\partial \bar{t}} + \bar{U} \frac{\partial}{\partial \bar{X}} + \bar{V} \frac{\partial}{\partial \bar{Y}} \right) \bar{V} = -\frac{\partial \bar{P}}{\partial \bar{Y}} + \frac{\partial}{\partial \bar{X}} (\Gamma_{\bar{Y}\bar{X}}) + \frac{\partial}{\partial \bar{Y}} (\Gamma_{\bar{Y}\bar{Y}}), \quad (7)$$

$$\rho C_p \left(\frac{\partial}{\partial t} + \bar{U} \frac{\partial}{\partial \bar{X}} + \bar{V} \frac{\partial}{\partial \bar{Y}} \right) \bar{T} = \bar{\nabla} \cdot (\bar{k}(\bar{T}) \bar{\nabla} \bar{T}) + \Gamma_{\bar{X}\bar{X}} \frac{\partial \bar{U}}{\partial \bar{X}} + \Gamma_{\bar{X}\bar{Y}} \frac{\partial \bar{U}}{\partial \bar{Y}} + \Gamma_{\bar{Y}\bar{X}} \frac{\partial \bar{V}}{\partial \bar{X}}. \quad (8)$$

In Eqs. (5)–(8), components $\Gamma_{\bar{X}\bar{Y}}$, $\Gamma_{\bar{Y}\bar{X}}$, $\Gamma_{\bar{Y}\bar{Y}}$ computed through the relations defined in Eqs. (2)–(4) are

$$\left\{ \begin{array}{l} \Gamma_{\bar{X}\bar{X}} = 2 \left(\bar{\mu}(\bar{T}) + \frac{\tau_y}{|\bar{\gamma}|} (1 - e^{-G^* |\bar{\gamma}|}) \right) \frac{\partial \bar{U}}{\partial \bar{X}}, \\ \Gamma_{\bar{X}\bar{Y}} = \Gamma_{\bar{Y}\bar{X}} = \left(\bar{\mu}(\bar{T}) + \frac{\tau_y}{|\bar{\gamma}|} (1 - e^{-G^* |\bar{\gamma}|}) \right) \left(\frac{\partial \bar{U}}{\partial \bar{Y}} + \frac{\partial \bar{V}}{\partial \bar{X}} \right), \\ \Gamma_{\bar{Y}\bar{Y}} = 2 \left(\bar{\mu}(\bar{T}) + \frac{\tau_y}{|\bar{\gamma}|} (1 - e^{-G^* |\bar{\gamma}|}) \right) \frac{\partial \bar{V}}{\partial \bar{Y}}, \\ |\bar{\gamma}| = \sqrt{2 \left(\frac{\partial \bar{U}}{\partial \bar{X}} \right)^2 + \left(\frac{\partial \bar{U}}{\partial \bar{Y}} + \frac{\partial \bar{V}}{\partial \bar{X}} \right)^2 + 2 \left(\frac{\partial \bar{V}}{\partial \bar{Y}} \right)^2} \end{array} \right. \quad (9)$$

In wave frame, using the transformations.

$$\left\{ \begin{array}{l} \bar{X} = \bar{x} + c\bar{t} \\ \bar{Y} = \bar{y} \\ \bar{U}(\bar{X}, \bar{Y}, \bar{t}) = \bar{u}(\bar{x}, \bar{y}) + c \\ \bar{V}(\bar{X}, \bar{Y}, \bar{t}) = \bar{v}(\bar{x}, \bar{y}) \\ \bar{P}(\bar{X}, \bar{Y}, \bar{t}) = \bar{p}(\bar{x}, \bar{y}) \\ \bar{T}(\bar{X}, \bar{Y}, \bar{t}) = T(\bar{x}, \bar{y}) \end{array} \right. , \quad (10)$$

Equations (5)–(8) becomes

$$\frac{\partial \bar{u}}{\partial \bar{x}} + \frac{\partial \bar{v}}{\partial \bar{y}} = 0, \quad (11)$$

$$\rho \left[\bar{u} \frac{\partial \bar{u}}{\partial \bar{x}} + \bar{v} \frac{\partial}{\partial \bar{y}} \right] = -\frac{\partial \bar{p}}{\partial \bar{x}} + \frac{\partial}{\partial \bar{x}} (\Gamma_{\bar{x}\bar{x}}) + \frac{\partial}{\partial \bar{y}} (\Gamma_{\bar{x}\bar{y}}), \quad (12)$$

$$\rho \left[\bar{u} \frac{\partial \bar{v}}{\partial \bar{x}} + \bar{v} \frac{\partial \bar{v}}{\partial \bar{y}} \right] = -\frac{\partial \bar{p}}{\partial \bar{y}} + \frac{\partial}{\partial \bar{x}} (\Gamma_{\bar{y}\bar{x}}) + \frac{\partial}{\partial \bar{y}} (\Gamma_{\bar{y}\bar{y}}), \quad (13)$$

$$\begin{aligned} \rho C_p \left[(\bar{u} + c) \frac{\partial T}{\partial \bar{x}} + \bar{v} \frac{\partial T}{\partial \bar{y}} \right] \theta &= \frac{\partial}{\partial \bar{x}} \left[k_0 \{ 1 + \gamma^*(T - T_0) \} \frac{\partial T}{\partial \bar{x}} \right] \\ &+ \frac{\partial}{\partial \bar{y}} \left[k_0 \{ 1 + \gamma^*(T - T_0) \} \frac{\partial T}{\partial \bar{y}} \right] \\ &+ \left[\Gamma_{\bar{x}\bar{x}} \frac{\partial \bar{u}}{\partial \bar{x}} + \Gamma_{\bar{x}\bar{y}} \frac{\partial \bar{u}}{\partial \bar{y}} + \Gamma_{\bar{y}\bar{x}} \frac{\partial \bar{v}}{\partial \bar{x}} + \Gamma_{\bar{y}\bar{y}} \frac{\partial \bar{v}}{\partial \bar{y}} \right], \end{aligned} \quad (14)$$

$$\left\{ \begin{array}{l} \Gamma_{\bar{x}\bar{x}} = 2 \left(\bar{\mu}(\bar{T}) + \frac{\tau_y}{|\bar{\gamma}|} (1 - e^{-G^*|\bar{\gamma}|}) \right) \frac{\partial \bar{u}}{\partial \bar{x}}, \\ \Gamma_{\bar{x}\bar{y}} = \left(\bar{\mu}(\bar{T}) + \frac{\tau_y}{|\bar{\gamma}|} (1 - e^{-G^*|\bar{\gamma}|}) \right) \left(\frac{\partial \bar{u}}{\partial \bar{y}} + \frac{\partial \bar{v}}{\partial \bar{x}} \right), \\ \Gamma_{\bar{y}\bar{y}} = 2 \left(\bar{\mu}(\bar{T}) + \frac{\tau_y}{|\bar{\gamma}|} (1 - e^{-G^*|\bar{\gamma}|}) \right) \frac{\partial \bar{v}}{\partial \bar{y}}, \\ |\bar{\gamma}| = \sqrt{2 \left(\frac{\partial \bar{u}}{\partial \bar{x}} \right)^2 + \left(\frac{\partial \bar{u}}{\partial \bar{y}} + \frac{\partial \bar{v}}{\partial \bar{x}} \right)^2 + 2 \left(\frac{\partial \bar{v}}{\partial \bar{y}} \right)^2}, \end{array} \right. \quad (15)$$

Introducing the following dimensionless numbers to decrease the number of independent variables utilized in the physical system

$$\left. \begin{array}{l} x = \frac{\bar{x}}{\lambda}, y = \frac{\bar{y}}{L_1}, u = \frac{\bar{u}}{c}, v = \frac{\bar{v}}{c\delta}, \delta = \frac{L_1}{\lambda}, p = \frac{\bar{p}}{\lambda c \mu_0 / L_1^2}, \\ Re = \frac{\rho c L_1}{\mu_0}, \Gamma_{xx} = \frac{\lambda}{\eta_0 c} \Gamma_{\bar{x}\bar{x}}, \Gamma_{yy} = \frac{L_1}{\eta_0 c} \Gamma_{\bar{y}\bar{y}}, \Gamma_{xy} = \frac{L_1}{\eta_0 c} \Gamma_{\bar{x}\bar{y}}, \\ B_n = \frac{\tau_y L_1}{c \mu_0}, G = \frac{G^* c}{L_1}, \alpha = \alpha^* (T_1 - T_0), \gamma = \gamma^* (T_1 - T_0), \\ \theta = \frac{T - T_0}{T_1 - T_0}, Pr = \frac{\mu_0 C_p}{k_0}, Ec = \frac{c^2}{C_p (T_1 - T_0)}, Br = \frac{\mu c^2}{k_0 (T_1 - T_0)}. \end{array} \right\} \quad (16)$$

Utilizing quantities (14) in Eqs. (11)–(15) gives the following dimensionless equations.

$$\delta \frac{\partial u}{\partial x} + \delta \frac{\partial v}{\partial y} = 0, \quad (17)$$

$$Re \delta \left[u \frac{\partial}{\partial x} + v \frac{\partial}{\partial y} \right] u = -\frac{\partial p}{\partial x} + \delta^2 \frac{\partial}{\partial x} (\Gamma_{xx}) + \frac{\partial}{\partial y} (\Gamma_{xy}), \quad (18)$$

$$Re \delta^3 \left[u \frac{\partial v}{\partial x} + v \frac{\partial v}{\partial y} \right] = -\frac{\partial p}{\partial y} + \delta^2 \frac{\partial}{\partial x} (\Gamma_{yx}) + \delta \frac{\partial}{\partial y} (\Gamma_{xy}), \quad (19)$$

$$\begin{aligned} Pr Re \delta \left[(u + 1) \frac{\partial \theta}{\partial x} + v \frac{\partial \theta}{\partial y} \right] &= \delta \frac{\partial}{\partial \eta} \left[(1 + \gamma \theta) \frac{\partial \theta}{\partial x} \right] + \frac{\partial}{\partial y} \left[(1 + \gamma \theta) \frac{\partial \theta}{\partial y} \right] \\ &+ Br \left[\delta^2 \Gamma_{xx} \frac{\partial u}{\partial x} + \Gamma_{xy} \frac{\partial u}{\partial y} + \delta^2 \Gamma_{yx} \frac{\partial v}{\partial y} + \delta \Gamma_{yy} \frac{\partial v}{\partial y} \right], \end{aligned} \quad (20)$$

$$\left\{ \begin{array}{l} \Gamma_{xx} = 2 \left(\mu(\theta) + \frac{B_n}{\Upsilon} (1 - e^{-G\Upsilon}) \right) \frac{\partial u}{\partial x}, \\ \Gamma_{xy} = \left(\mu(\theta) + \frac{B_n}{\Upsilon} (1 - e^{-G\Upsilon}) \right) \left(\frac{\partial u}{\partial y} + \delta \frac{\partial v}{\partial x} \right), \\ \Gamma_{yy} = 2 \left(\mu(\theta) + \frac{B_n}{\Upsilon} (1 - e^{-G\Upsilon}) \right) \frac{\partial v}{\partial y}, \\ \Upsilon = \sqrt{2\delta^2 \left(\frac{\partial u}{\partial x} \right)^2 + \left(\frac{\partial u}{\partial y} + \delta \frac{\partial v}{\partial x} \right)^2 + 2\delta^2 \left(\frac{\partial v}{\partial y} \right)^2}, \end{array} \right.$$

In terms of stream function

$$u = \frac{\partial \psi}{\partial y}, \quad v = -\frac{\partial \psi}{\partial x} \quad (21)$$

Equations (16)–(20) takes the form

$$\delta \frac{\partial^2 \psi}{\partial x \partial y} - \delta \frac{\partial^2 \psi}{\partial y \partial x} = 0, \quad (22)$$

$$\text{Re} \delta \left[\frac{\partial \psi}{\partial y} \frac{\partial}{\partial x} - \frac{\partial \psi}{\partial x} \frac{\partial}{\partial y} \right] \frac{\partial \psi}{\partial y} = -\frac{\partial p}{\partial x} + \delta^2 \frac{\partial}{\partial x} (\Gamma_{xx}) + \frac{\partial}{\partial y} (\Gamma_{xy}), \quad (23)$$

$$-\text{Re} \delta^3 \left[\frac{\partial \psi}{\partial y} \frac{\partial}{\partial x} - \frac{\partial \psi}{\partial x} \frac{\partial}{\partial y} \right] \frac{\partial \psi}{\partial x} = -\frac{\partial p}{\partial y} + \delta^2 \frac{\partial}{\partial x} (\Gamma_{yx}) + \delta \frac{\partial}{\partial y} (\Gamma_{xy}), \quad (24)$$

$$\begin{aligned} \text{Pr Re} \delta \left[\left(\frac{\partial \psi}{\partial y} + 1 \right) \frac{\partial \theta}{\partial x} - \frac{\partial \psi}{\partial x} \frac{\partial \theta}{\partial y} \right] &= \delta \frac{\partial}{\partial \eta} \left[(1 + \gamma \theta) \frac{\partial \theta}{\partial x} \right] + \frac{\partial}{\partial y} \left[(1 + \gamma \theta) \frac{\partial \theta}{\partial y} \right] \\ &+ Br \left[\delta^2 \Gamma_{xx} \frac{\partial u}{\partial x} + \Gamma_{xy} \frac{\partial u}{\partial y} + \delta^2 \Gamma_{yx} \frac{\partial v}{\partial y} + \delta \Gamma_{yy} \frac{\partial v}{\partial y} \right], \end{aligned} \quad (25)$$

$$\left\{ \begin{array}{l} \Gamma_{xx} = 2 \left(\mu(\theta) + \frac{B_n}{\Upsilon} (1 - e^{-G\Upsilon}) \right) \frac{\partial^2 \psi}{\partial x \partial y}, \\ \Gamma_{xy} = \left(\mu(\theta) + \frac{B_n}{\Upsilon} (1 - e^{-G\Upsilon}) \right) \left(\frac{\partial^2 \psi}{\partial y^2} - \delta \frac{\partial^2 \psi}{\partial x^2} \right), \\ \Gamma_{yy} = -2 \left(\mu(\theta) + \frac{B_n}{\Upsilon} (1 - e^{-G\Upsilon}) \right) \frac{\partial^2 \psi}{\partial x \partial y}, \\ \Upsilon = \sqrt{2\delta^2 \left(\frac{\partial^2 \psi}{\partial x \partial y} \right)^2 + \left(\frac{\partial^2 \psi}{\partial y^2} - \delta \frac{\partial^2 \psi}{\partial x^2} \right)^2 + 2\delta^2 \left(\frac{\partial^2 \psi}{\partial x \partial y} \right)^2}, \end{array} \right. \quad (26)$$

Supposition of small Reynolds number ($\text{Re} \approx 0$) and long wavelength ($\delta \approx 0$), the continuity equation is automatically fulfilled, and Eqs. (22)–(26) are simplified to:

$$\frac{\partial p}{\partial y} = 0, \quad (27)$$

$$\frac{\partial p}{\partial x} = \frac{\partial}{\partial y} [\Gamma_{xy}], \quad (28)$$

$$\frac{\partial}{\partial y} \left[k(\theta) \frac{\partial \theta}{\partial y} \right] + Br \left[\Gamma_{xy} \frac{\partial^2 \psi}{\partial y^2} \right], \quad (29)$$

$$\Gamma_{xy} = \left(\mu(\theta) + \frac{B_n}{\Upsilon} (1 - e^{-G\Upsilon}) \right) \left(\frac{\partial^2 \psi}{\partial y^2} \right), \quad (30)$$

$$\Upsilon = \frac{\partial^2 \psi}{\partial y^2}.$$

From Eqs. (27) and (28) after elimination pressure gradient we have

$$\frac{\partial}{\partial y} \left[\frac{\partial}{\partial y} \left(\mu(\theta) \frac{\partial^2 \psi}{\partial y^2} \right) + B_n G \left(\frac{\partial^3 \psi}{\partial y^3} \right) e^{-G \frac{\partial^2 \psi}{\partial y^2}} \right] = 0, \quad (31)$$

$$\frac{\partial}{\partial y} \left(k(\theta) \frac{\partial \theta}{\partial y} \right) + Br \left(\mu(\theta) \left(\frac{\partial^2 \psi}{\partial y^2} \right)^2 + B_n \left(1 - e^{-G \frac{\partial^2 \psi}{\partial y^2}} \right) \frac{\partial^2 \psi}{\partial y^2} \right) = 0 \quad (32)$$

Utilizing the relations of temperature-dependent properties defined in Refs. [44–48], Eqs. (31) and (32) takes the form:

$$\frac{\partial}{\partial y} \left[\frac{\partial}{\partial y} \left((1 - \alpha\theta) \frac{\partial^2 \psi}{\partial y^2} \right) + GB_n \left(\frac{\partial^3 \psi}{\partial y^3} \right) e^{-G \frac{\partial^2 \psi}{\partial y^2}} \right] = 0, \quad (33)$$

$$\frac{\partial}{\partial y} \left((1 + \gamma\theta) \frac{\partial \theta}{\partial y} \right) + Br \left((1 - \alpha\theta) \left(\frac{\partial^2 \psi}{\partial y^2} \right)^2 + B_n \left(1 - e^{-G \frac{\partial^2 \psi}{\partial y^2}} \right) \frac{\partial^2 \psi}{\partial y^2} \right) = 0 \quad (34)$$

In laboratory frame (fixed frame) and in the wave frame (moving frame) the volume flow rate \bar{Q} and q are respectively, defined by

$$\bar{Q} = \int_{\bar{h}_2(\bar{x}, \bar{t})}^{\bar{h}_1(\bar{x}, \bar{t})} \bar{U}(\bar{X}, \bar{Y}, \bar{t}) d\bar{Y}. \quad (35)$$

$$q = \int_{\bar{h}_2(\bar{x})}^{\bar{h}_1(\bar{x})} \bar{u}(\bar{x}, \bar{y}) d\bar{y}. \quad (36)$$

From Eqs. (35) and (36) we obtain

$$\bar{Q} = q + c(\bar{h}_1 - \bar{h}_2). \quad (37)$$

The time averaged flow over a period P^* at a fixed position \bar{X} is defined as

$$Q^* = \frac{1}{P^*} \int_0^{P^*} \bar{Q} dt. \quad (38)$$

Utilizing Eq. (37) in (38) leads to the following result:

$$Q^* = q + c(L_1 + L_2). \quad (39)$$

Non-dimensional time-mean flows Q and F are

$$Q = \frac{Q^*}{cL_1}, \quad F = \frac{q}{cL_1}. \quad (40)$$

Therefore, we can establish the following relationship between the flow rates:

$$Q = F + 1 + L. \quad (41)$$

Also, from (36) we can define the dimensionless mean flow rate in terms of stream function as

$$F = \int_{h_2(x)}^{h_1(x)} \frac{\partial \psi}{\partial y} dy = \psi(h_1) - \psi(h_2). \quad (42)$$

The appropriate boundary conditions are as follows:

$$\begin{cases} \psi = -\frac{F}{2}, & \frac{\partial\psi}{\partial y} = -1, & \theta = 1 & \text{at } y = h_2 = -L - B\cos(2\pi x + \phi), \\ \psi = +\frac{F}{2}, & \frac{\partial\psi}{\partial y} = -1, & \theta = 0 & \text{at } y = h_1 = 1 + A\cos(2\pi x). \end{cases} \quad (43)$$

For a two-dimensional flow of an incompressible and dissipative Bingham-Papanastasiou fluid, the rate of entropy formation can be expressed as follows:

$$\dot{S}_{gen}''' = \frac{\bar{\kappa}(\bar{T})}{\bar{T}^2} \left[\left(\frac{\partial\bar{T}}{\partial\bar{X}} \right)^2 + \left(\frac{\partial\bar{T}}{\partial\bar{Y}} \right)^2 \right] + \frac{\mu(\bar{T})}{\bar{T}} \left[\begin{aligned} &\Gamma_{\bar{X}\bar{X}} \frac{\partial\bar{U}}{\partial\bar{X}} + \Gamma_{\bar{X}\bar{Y}} \frac{\partial\bar{U}}{\partial\bar{Y}} \\ &+ \Gamma_{\bar{Y}\bar{X}} \frac{\partial\bar{V}}{\partial\bar{X}} + \Gamma_{\bar{Y}\bar{Y}} \frac{\partial\bar{V}}{\partial\bar{Y}} \end{aligned} \right] \quad (44)$$

In dimensionless form, after applying above stated transformations and assumptions Eq. (44) becomes:

$$Ns = \frac{\dot{S}_{gen}'''}{S_{go}'''} = \frac{(1 + \gamma\theta)}{(\theta + \Lambda)^2} \left(\frac{\partial\theta}{\partial y} \right)^2 + \frac{Br}{(\theta + \Lambda)} \left[(1 - \alpha\theta) \left(\frac{\partial^2\psi}{\partial y^2} \right)^2 + B_n \left(1 - e^{-G \frac{\partial^2\psi}{\partial y^2}} \right) \frac{\partial^2\psi}{\partial y^2} \right]. \quad (45)$$

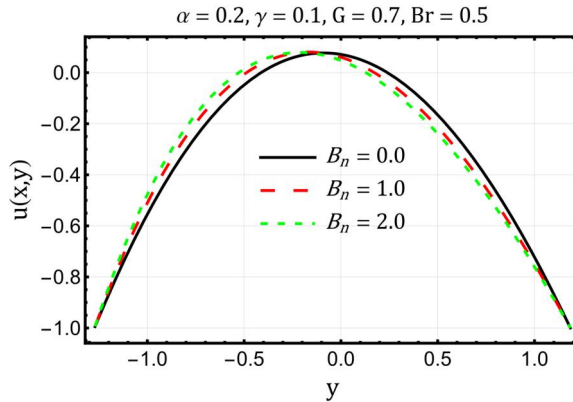


Figure 1. Velocity profiles $u(x,y)$ for Bingham number B_n .

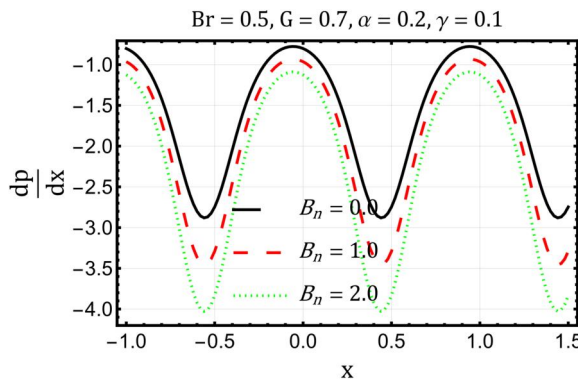


Figure 2. Axial pressure gradient profiles $\frac{dp}{dx}$ for Bingham number B_n .

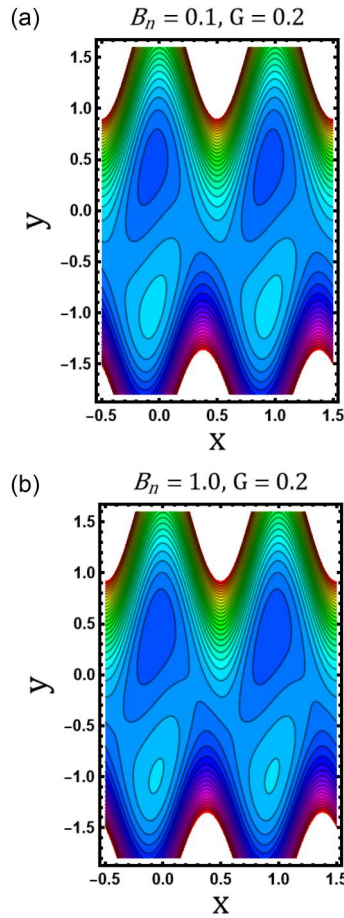


Figure 3. (a): Trapping phenomena when Bingham number $B_n(=0.1)$. (b) Trapping phenomena when Bingham number $B_n(=1.0)$.

3. Graphical presentation and interpretation

This section is dedicated to the investigation of alterations in the behavior of fluid flow $u(x, y)$, axial pressure gradient $\frac{dp}{dx}$, heat transfer $\theta(x, y)$, entropy generation Ns , and the Bejan number Be across an expanding array of dimensionless parameters inherent in the flow phenomenon. The analysis of fluid flow is illustrated in Figure 1, depicting distinct values of the Bingham number B_n . It is evident that as the Bingham number B_n increases, the flow intensifies along the upper wall, while it diminishes in the vicinity of the lower wall region. Figure 2 is drawn to see the impact of Bingham number B_n on the axial pressure gradient $\frac{dp}{dx}$. Magnitude of the axial pressure gradient $\frac{dp}{dx}$ increases as the Bingham number B_n increases. With an increase in the Bingham fluid parameter (indicating higher yield stress), the fluid's tendency to initiate flow is reduced. This implies that a greater external force or stress must be applied to surpass the yield stress threshold and induce flow. The response of the fluid to pressure gradients is influenced by the yield stress. A higher yield stress necessitates a greater pressure gradient to originate the flow. As the yield stress elevates, the fluid's resistance to flow intensifies, demanding a more robust pressure gradient to surmount this resistance and prompt flow. Figure 3 is designed to show the effects of the Bingham number on the temperature profile, it is seen that the heat flow

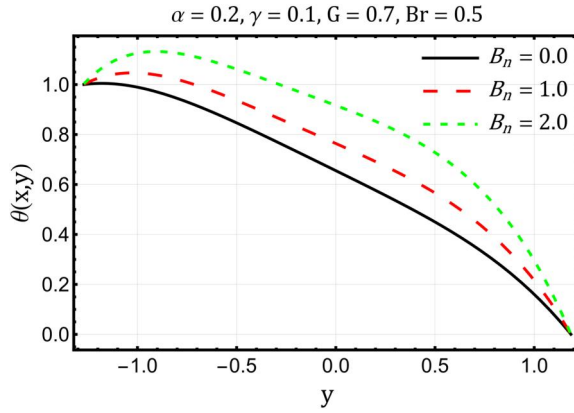


Figure 4. Temperature profiles $\theta(x,y)$ for Bingham number B_n .

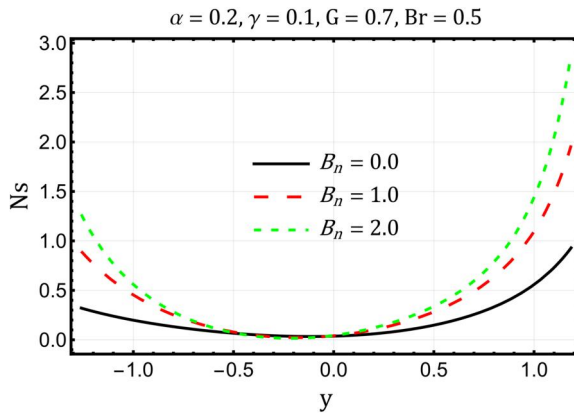


Figure 5. Entropy generation number profiles N_s for Bingham number B_n .

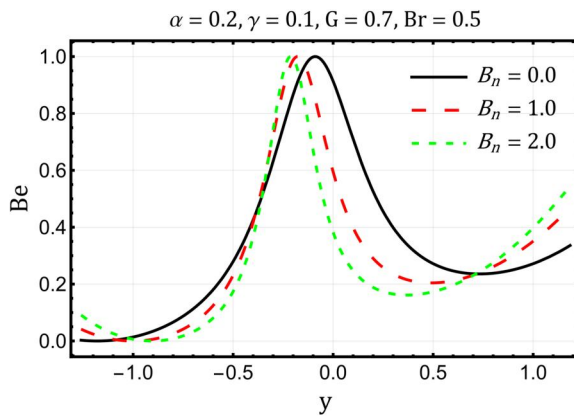


Figure 6. Entropy generation number profiles Be for Bingham number B_n .

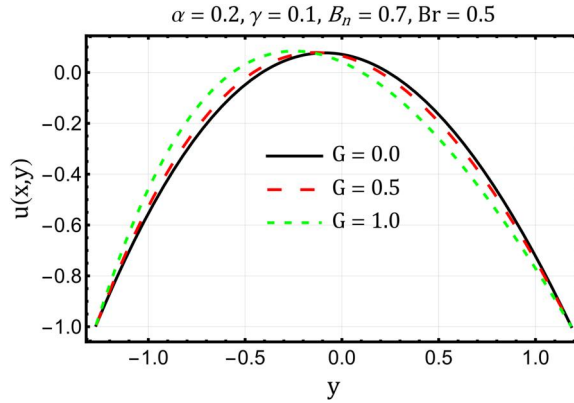


Figure 7. Velocity profiles $u(x,y)$ for stress growth component G .

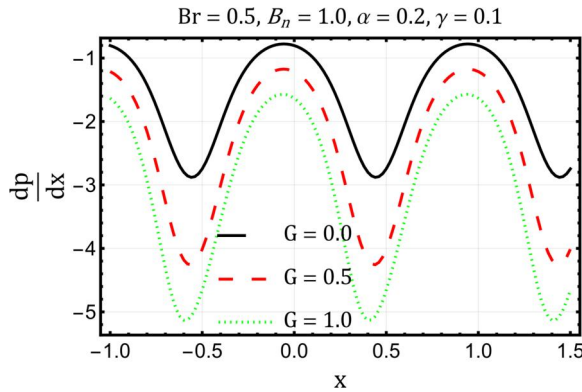


Figure 8. Axial pressure gradient profiles $\frac{dp}{dx}$ for stress growth component G .

decreases with the increase of the Bingham number B_n . Effect of Bingham number on the streamlines pattern is plotted in Figure 4(a, b), inside the conduit it is observed through this graph that the number of boluses is increasing on the increase of Bingham number; this is natural because Bingham number describes the amount of fluid motion. The effect of Bingham number on entropy generation is plotted in Figure 5, it is seen that entropy is proactive near the channel walls, however, stable and minimum at the center. For the analysis of Bejan number under the influence of Bingham number is displayed in Figure 6. The ratio of heat generated entropy to entropy generated by other factors affecting fluid flow is known as Bejan number. Bejan number is observed to be constantly rising along with Bingham number, but it changes after reaching its maximum value and begins to fall close to the channel's upper wall. Figures 7–12 are portrayed to capture the variation of nondimensional stress growth parameter G on velocity $u(x,y)$, axial pressure gradient $\frac{dp}{dx}$ trapping phenomena $\psi(x,y)$, heat transfer $\theta(x,y)$, entropy generation (Ns), and the Bejan number (Be) The impact of stress growth parameter G on all the aforementioned fields is qualitatively similar to the Bingham number B_n . In Figures 13 and 14, we analyzed the dimensionless shear stress with increasing values of B_n and stress growth component G . We observed from these figures that dimensionless shear stress Γ_{xy} has increasing behavior with large values of B_n and stress growth component G . Figures 15 and 16 respectively, portrayed the

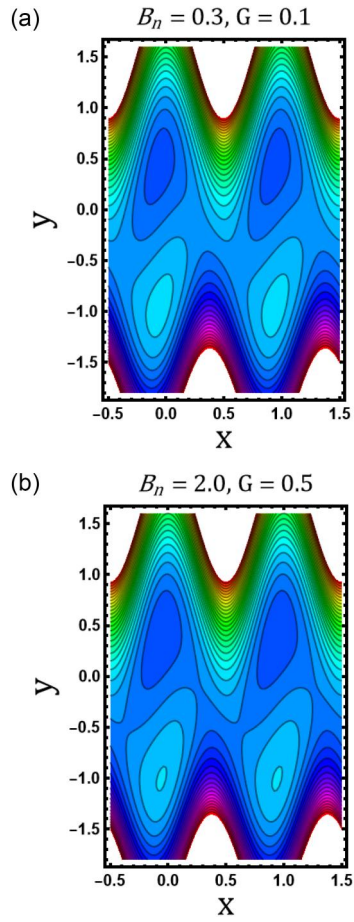


Figure 9. (a) Trapping phenomena when stress growth component $G(= 0.1)$. (b) Trapping phenomena when stress growth component $G(= 0.5)$.

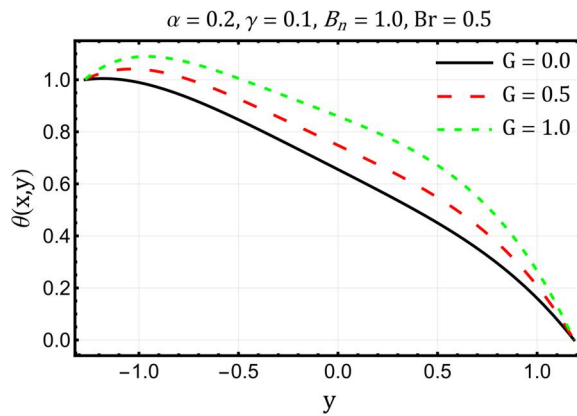


Figure 10. Temperature profiles $\theta(x,y)$ for stress growth component G .

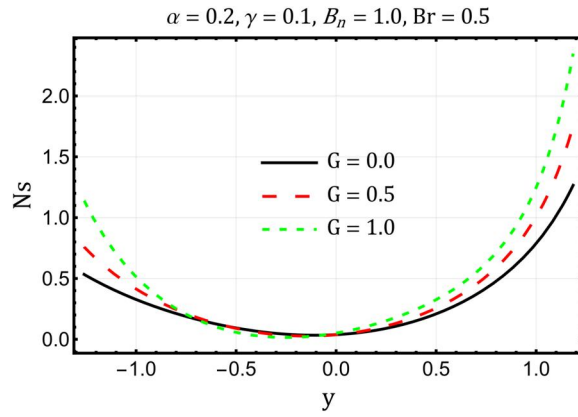


Figure 11. Entropy generation number profiles N_s for stress growth component G .

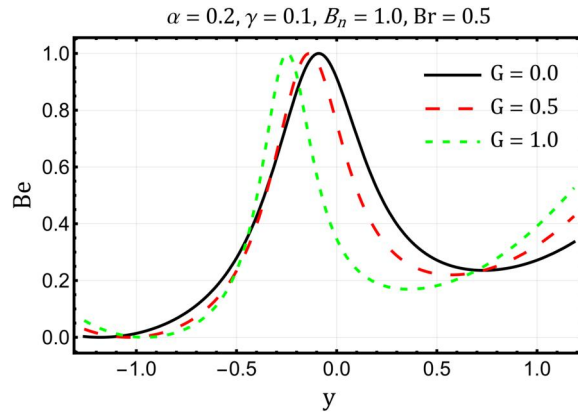


Figure 12. Bejan number profiles Be for stress growth component G .

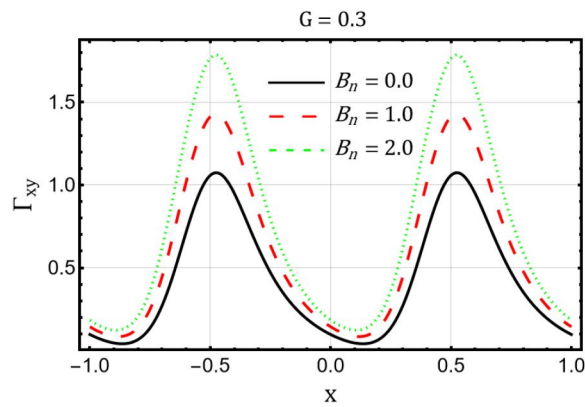


Figure 13. Dimensionless shear stress Γ_{xy} for Bingham number B_n .

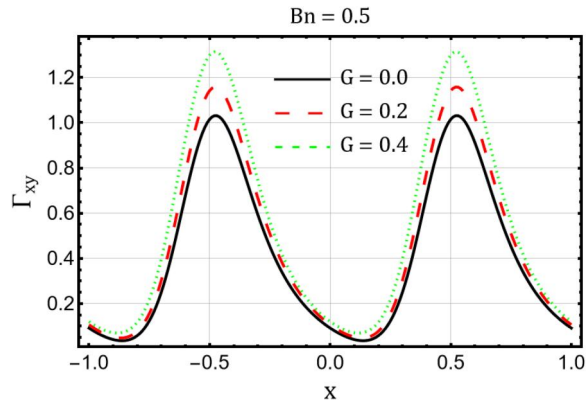


Figure 14. Dimensionless shear stress Γ_{xy} for stress growth component G .

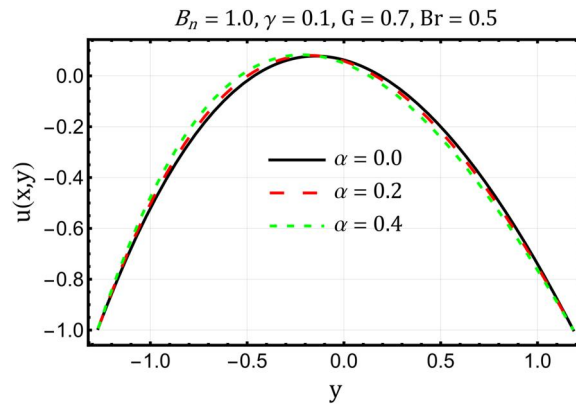


Figure 15. Velocity profiles $u(x,y)$ for variable viscosity parameter α .

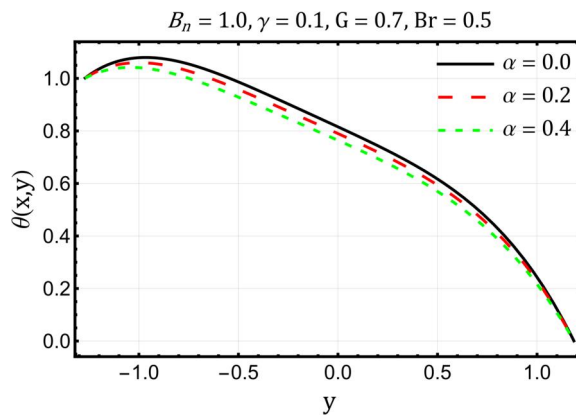


Figure 16. Temperature profiles $\theta(x,y)$ for variable viscosity parameter α .

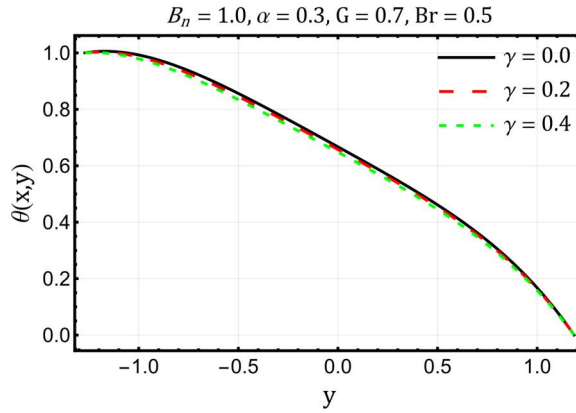


Figure 17. Temperature profiles $\theta(x,y)$ for variable thermal conductivity parameter γ .

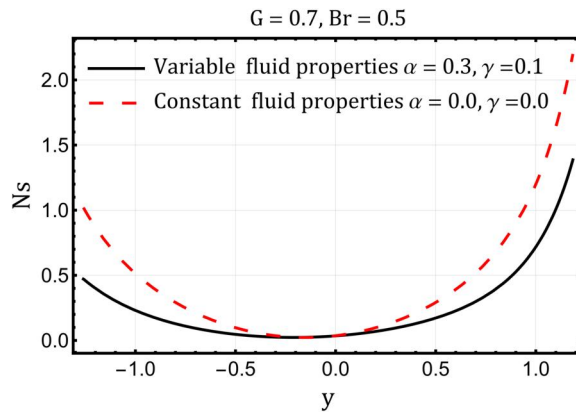


Figure 18. Comparison of entropy generation number Ns for cases of constant and variable fluid properties.

variation in velocity $u(x,y)$ and temperature $\theta(x,y)$ profiles for different values of variable viscosity α . It is noticed that the velocity decreases but increases later. Figure 16 shows that the temperature of fluid decreases by increasing viscosity parameter. Figure 17 depicts that the temperature of fluid also decreases by increasing the variable thermal conductivity parameter. Figure 18 is plotted to see the variation in entropy for the cases of constant and variable properties. Entropy generation substantially changes when the viscosity and thermal conductivity are assumed to be temperature dependent.

4. Conclusions

Entropy analysis of a Bingham-Papanastasiou fluid in an asymmetric channel is performed in this article. The investigation also considers the viscous dissipation of the fluid in the context of thermal analysis. The study yields specific outcomes, which are emphasized as follows:

- All relevant physical quantities exhibit similarity in response to variations in stress growth parameter and the Bingham number.
- The fluid's velocity adjacent to the walls exhibits a contrasting behavior.
- As both the Bingham number and stress growth increase, the temperature distribution also experiences a rise.

- The magnitude of the pressure gradient rises with a rise in the stress growth rate parameter.
- Dimensionless shear stress also increases by increasing Bingham number.
- Entropy displays an active behavior in the proximity of the channel walls, while remaining stable and minimized at the central region.

Disclosure statement

No potential conflict of interest was reported by the author(s).

ORCID

Muhammad Idrees Afridi  <http://orcid.org/0000-0002-8818-5980>

Ali J. Chamkha  <http://orcid.org/0000-0002-8335-3121>

References

- [1] T. W. Latham, "Fluid motion in a peristaltic pump," MS thesis, Massachusetts Institute of Technology, Cambridge, 1966.
- [2] R. P. Chhabra and J. F. Richardson, *Non-Newtonian Flow; Fundamentals and Engineering Application*. Oxford: Butterworth-Heinemann, 1999.
- [3] G. R. Cokelet, *The Rheology of Human Blood*. Englewood Cliffs, NJ: Prentice-Hall, 1972,
- [4] F. Irgens, *Rheology and Non-Newtonian Fluids*. Cham: Springer, 2013.
- [5] A. Wu, *Rheology of Paste in Metal Mines*. Singapore: Springer, 2022.
- [6] M. G. Reddy and K. V. Reddy, "Influence of Joule heating on MHD peristaltic flow of a nanofluid with compliant walls," *Proc. Eng.*, vol. 127, pp. 1002–1009, 2015. DOI: [10.1016/j.proeng.2015.11.449](https://doi.org/10.1016/j.proeng.2015.11.449).
- [7] M. G. Reddy and O. D. Makinde, "Magnetohydrodynamic peristaltic transport of Jeffrey nanofluid in an asymmetric channel," *J. Molecular Liquids.*, vol. 223, pp. 1242–1248, 2016. DOI: [10.1016/j.molliq.2016.09.080](https://doi.org/10.1016/j.molliq.2016.09.080).
- [8] S. Mosayebidorcheh and M. Hatami, "Analytical investigation of peristaltic nanofluid flow and heat transfer in an asymmetric wavy wall channel (Part I: straight channel)," *Int. J. Heat Mass Transf.*, vol. 126, pp. 790–799, 2018. DOI: [10.1016/j.ijheatmasstransfer.2018.05.080](https://doi.org/10.1016/j.ijheatmasstransfer.2018.05.080).
- [9] N. K. Ranjit, G. C. Shit and D. Tripathi, "Joule heating and zeta potential effects on peristaltic blood flow through porous micro vessels altered by electrohydrodynamic," *Microvasc. Res.*, vol. 117, pp. 74–89, 2018. DOI: [10.1016/j.mvr.2017.12.004](https://doi.org/10.1016/j.mvr.2017.12.004).
- [10] D. Jing and M. Hatami, "Peristaltic Carreau-Yasuda nanofluid flow and mixed heat transfer analysis in an asymmetric vertical and tapered wavy wall channel," *Rep. Mech. Eng.*, vol. 1, no. 1, pp. 128–140, 2020. DOI: [10.31181/rme200101128h](https://doi.org/10.31181/rme200101128h).
- [11] K. Ramesh, D. Tripathi, M. M. Bhatti and C. M. Khalique, "Electro-osmotic flow of hydromagnetic dusty viscoelastic fluids in a microchannel propagated by peristalsis," *J. Molecular Liquids.*, vol. 314, pp. 113568, 2020. DOI: [10.1016/j.molliq.2020.113568](https://doi.org/10.1016/j.molliq.2020.113568).
- [12] D. S. Bhandari, D. Tripathi and V. K. Narla, "Magnetohydrodynamics-based pumping flow model with propagative rhythmic membrane contraction," *Eur. Phys. J. Plus*, vol. 135, pp. 890, 2020.
- [13] G. K. Ramesh, K. G. Kumar, A. J. Chamkha and R. S. R. Gorla, "Effects of chemical reaction and activation energy on a Carreau nano liquid past a permeable surface under zero mass flux conditions," *Proc. Inst. Mech. Eng. N J. Nanomater. Nanoeng. Nanosyst.*, vol. 234, no. 1-2, pp. 47–57, 2020. DOI: [10.1177/2397791419881090](https://doi.org/10.1177/2397791419881090).
- [14] D. S. Bhandari, D. Tripathi and O. Anwar Bég, "Electro-osmosis modulated periodic membrane pumping flow and particle motion with magnetic field effects," *Phys. Fluids.*, vol. 34, no. 9, pp. 092014, 2022. DOI: [10.1063/5.0111050](https://doi.org/10.1063/5.0111050).
- [15] G. H. R. Kefayati and R. R. Huilgol, "Lattice Boltzmann Method for simulation of mixed convection of a Bingham fluid in a lid-driven cavity," *Int. J. Heat Mass Transf.*, vol. 103, pp. 725–743, 2016. DOI: [10.1016/j.ijheatmasstransfer.2016.07.102](https://doi.org/10.1016/j.ijheatmasstransfer.2016.07.102).
- [16] J. Zhang, R. E. Khayat and A. P. Noronha, "Three-dimensional lubrication flow of a Herschel-Bulkley fluid," *Int. J. Numer. Meth. Fluids*, vol. 50, no. 4, pp. 511–530, 2006. DOI: [10.1002/flid.1076](https://doi.org/10.1002/flid.1076).
- [17] M. Nakamura and T. Sawada, "Numerical study on the flow of a non-Newtonian fluid through an axisymmetric stenosis," *J. Biomech. Eng.*, vol. 110, no. 2, pp. 137–143, 1988. DOI: [10.1115/1.3108418](https://doi.org/10.1115/1.3108418).

- [18] E. C. Bingham, "An investigation of the laws of plastic flow," *Bull. Natl. Bur. Stand.*, vol. 13, no. 2, pp. 309–353, 2018. DOI: [10.6028/bulletin.304](https://doi.org/10.6028/bulletin.304).
- [19] L. Fusi and A. Farina, "Flow of a Bingham fluid in a non-symmetric inclined channel," *J. Non-Newtonian Fluid Mech.*, vol. 238, pp. 24–32, 2016. DOI: [10.1016/j.jnnfm.2016.04.007](https://doi.org/10.1016/j.jnnfm.2016.04.007).
- [20] T. C. Papanastasiou, "Flows of materials with yield," *J. Rheol.*, vol. 31, no. 5, pp. 385–404, 1987. DOI: [10.1122/1.549926](https://doi.org/10.1122/1.549926).
- [21] T. C. Papanastasiou and A. G. Boudouvis, "Flows of viscoplastic materials: models and computations," *Comput. Struct.* vol. 64, no. 1–4, pp. 677–694, 1997. DOI: [10.1016/S0045-7949\(96\)00167-8](https://doi.org/10.1016/S0045-7949(96)00167-8).
- [22] H. Zhu, Y. D. Kim and D. DeKee, "Non-Newtonian fluids with a yield stress," *J. Non-Newtonian Fluid Mec.*, vol. 129, no. 3, pp. 177–181, 2005. DOI: [10.1016/j.jnnfm.2005.06.001](https://doi.org/10.1016/j.jnnfm.2005.06.001).
- [23] A. Mehmood, R. Mahmood, A. H. Majeed and F. J. Awan, "Flow of the Bingham-Papanastasiou regularized material in a channel in the presence of obstacles: correlation between hydrodynamic forces and spacing of obstacles," *Modell. Simul. Eng.*, vol. 2021, pp. 1–14, 2021. DOI: [10.1155/2021/5583110](https://doi.org/10.1155/2021/5583110).
- [24] Z. You, R. R. Huilgol and E. Mitsoulis, "Application of the Lambert W function to steady shearing flows of the Papanastasiou model," *Int. J. Eng. Sci.*, vol. 46, no. 8, pp. 799–808, 2008. DOI: [10.1016/j.ijengsci.2008.02.002](https://doi.org/10.1016/j.ijengsci.2008.02.002).
- [25] H. P. Soto, M. L. Martins-Costa, C. Fonseca and S. Frey, "A numerical investigation of inertia flows of Bingham-Papanastasiou fluids by an extra stress-pressure-velocity Galerkin least-squares method," *J. Braz. Soc. Mech. Sci. Eng.*, vol. 32, no. spe, pp. 450–460, 2010. DOI: [10.1590/S1678-58782010000500004](https://doi.org/10.1590/S1678-58782010000500004).
- [26] G. Daniel, C. Yoan, P. Zoltan and P. Yves, "Bingham-Papanastasiou and approximate parallel models comparison for the design of magneto-rheological valves," presented at the International Conference on Advanced Intelligent Mechatronics, Besancon, France, 2014, pp. 168–173.
- [27] N. A. Khan and F. Sultan, "Numerical analysis for the Bingham-Papanastasiou fluid flow over a rotating disk," *J. Appl. Mech. Tech. Phys.*, vol. 59, no. 4, pp. 638–644, 2018. DOI: [10.1134/S0021894418040090](https://doi.org/10.1134/S0021894418040090).
- [28] E. Aitavade, S. Patil, A. Kadam and T. Mulla, "An overview of peristaltic pump suitable for handling of various slurries and liquids," *J. Mech. Civil Eng.*, vol. 2, pp. 19–24, 2012.
- [29] J. Cai, A. H. Azimi, D. Z. Zhu and N. Rajaratnam, "Experimental and numerical studies on pumping viscoplastic fluids," *Can. J. Civ. Eng.*, vol. 43, no. 8, pp. 675–684, 2016. DOI: [10.1139/cjce-2015-0500](https://doi.org/10.1139/cjce-2015-0500).
- [30] D. Tripathi and O. A. Bèg, "Mathematical modelling of peristaltic propulsion of viscoplastic bio-fluids," *Proc. Inst. Mech. Eng. H.*, vol. 228, no. 1, pp. 67–88, 2014. DOI: [10.1177/0954411913511584](https://doi.org/10.1177/0954411913511584).
- [31] F. Aslam and S. Noreen, "Electrokinetic peristaltic transport of Bingham-Papanastasiou fluid via porous media," *J. Appl. Math. Mech.*, vol. 104, no. 2, pp. e202300070, 2023. DOI: [10.1002/zamm.202300070](https://doi.org/10.1002/zamm.202300070).
- [32] A. Bejan, *Entropy Generation through Heat and Fluid Flow*. New York: Wiley, 1982.
- [33] A. Bejan, "Entropy generation minimization: the new thermodynamics of finite-size devices and finite-time processes," *J. Appl. Phys.*, vol. 79, no. 3, pp. 1191–1218, 1996. DOI: [10.1063/1.362674](https://doi.org/10.1063/1.362674).
- [34] O. D. Makinde and A. S. Eegunjobi, "Entropy generation in a couple stress fluid flow through a vertical channel filled with saturated porous media," *Entropy*, vol. 15, no. 12, pp. 4589–4606, 2013. DOI: [10.3390/e15114589](https://doi.org/10.3390/e15114589).
- [35] G. C. Shit and S. Mandal, "Entropy analysis on unsteady MHD flow of Casson nanofluid over a stretching vertical plate with thermal radiation effect," *Int. J. Appl. Comput. Math.*, vol. 6, no. 1, pp. 1–22, 2020. DOI: [10.1007/s40819-019-0754-4](https://doi.org/10.1007/s40819-019-0754-4).
- [36] M. I. Afridi, M. Qasim and S. Saleem, "Second law analysis of three-dimensional dissipative flow of hybrid nanofluid," *J. Nanofluids.*, vol. 7, no. 6, pp. 1272–1280, 2018. DOI: [10.1166/jon.2018.1532](https://doi.org/10.1166/jon.2018.1532).
- [37] M. I. Afridi and M. Qasim, "Entropy generation and heat transfer in boundary layer flow over a thin needle moving in a parallel stream in the presence of nonlinear Rosseland radiation," *Int. J. Therm. Sci.*, vol. 123, pp. 117–128, 2018. DOI: [10.1016/j.ijthermalsci.2017.09.014](https://doi.org/10.1016/j.ijthermalsci.2017.09.014).
- [38] M. Qasim, Z. H. Khan, I. Khan and Q. M. Al-Mdallal, "Analysis of entropy generation in flow of methanol-based nanofluid in a sinusoidal wavy channel," *Entropy*, vol. 19, no. 10, pp. 490, 2017. DOI: [10.3390/e19100490](https://doi.org/10.3390/e19100490).
- [39] K. Ranjit and G. C. Shit, "Entropy generation on electro-osmotic flow pumping by a uniform peristaltic wave under magnetic environment," *Energy*, vol. 128, pp. 649–660, 2017. DOI: [10.1016/j.energy.2017.04.035](https://doi.org/10.1016/j.energy.2017.04.035).
- [40] N. S. Akbar and A. W. Butt, "Entropy generation analysis for the peristaltic flow of Cu-water nanofluid in a tube with viscous dissipation," *J. Hydrodyn.*, vol. 29, no. 1, pp. 135–143, 2017. DOI: [10.1016/S1001-6058\(16\)60725-4](https://doi.org/10.1016/S1001-6058(16)60725-4).
- [41] H. Zahir, T. Hayat, A. Alsaedi and B. Ahmad, "Entropy generation impact on peristaltic motion in a rotating frame," *Results Phys.*, vol. 7, pp. 3668–3677, 2017. DOI: [10.1016/j.rinp.2017.09.045](https://doi.org/10.1016/j.rinp.2017.09.045).
- [42] N. Saleem, "Entropy production in peristaltic flow of a space dependent viscosity fluid in asymmetric channel," *Therm. Sci.*, vol. 22, no. 6 Part B, pp. 2909–2918, 2018. DOI: [10.2298/TSCI161020164S](https://doi.org/10.2298/TSCI161020164S).

- [43] V. K. Narla, K. M. Prasad and J. V. R. Murthy, "Second-law analysis of the peristaltic flow of an incompressible viscous fluid in a curved channel," *J. Eng. Phys. Thermophys.*, vol. 89, no. 2, pp. 441–448, 2016. DOI: [10.1007/s10891-016-1394-8](https://doi.org/10.1007/s10891-016-1394-8).
- [44] M. S. Reddy, M. V. V. Reddy, B. J. Reddy and S. R. Krishna, "Peristaltic pumping of Jeffery fluid with variable viscosity in a tube under the effect of magnetic field," *J. Math. Comput. Sci.*, vol. 2, pp. 907–925, 2012.
- [45] M. V. S. Reddy and D. P. Reddy, "Peristaltic pumping of a Jeffrey fluid with variable viscosity through a porous medium in a planar channel," *Int. J. Math. Arch.*, vol. 1, pp. 42–54, 2010.
- [46] K. S. Mekheimer and Y. A. Elmagboud, "Simultaneous effects of variable viscosity and thermal conductivity on peristaltic flow in a vertical asymmetric channel," *Can. J. Phys.*, vol. 92, no. 12, pp. 1541–1555, 2014. DOI: [10.1139/cjp-2013-0465](https://doi.org/10.1139/cjp-2013-0465).
- [47] Q. Hussain, S. Asghar, T. Hayat and A. Alsaedi A, "Peristaltic transport of hydromagnetic Jeffrey fluid with temperature dependent viscosity and thermal conductivity," *Int. J. Biomath.*, vol. 09, no. 02, pp. 1650029, 2016. DOI: [10.1142/S1793524516500297](https://doi.org/10.1142/S1793524516500297).
- [48] H. Vaidya, K.V. Prasad, M. I. Khan, F. Mebarek-Oudina, I. Tlili, C. Rajashekhar, N. Shivaleela, S. Elattar, M. I. Khan, S. G. Al-Gamdi, Combined effects of chemical reaction and variable thermal conductivity on MHD peristaltic flow of Phan-Thien-Tanner liquid through inclined channel, *Case Stud. Therm. Eng.*, vol. 36, pp. 102214, 2022. DOI: [10.1016/j.csite.2022.102214](https://doi.org/10.1016/j.csite.2022.102214).
- [49] M. Qasim, Z. Ali, U. Farooq and D. Lu, "Investigation of entropy in two-dimensional peristaltic flow with temperature dependent viscosity, thermal and electrical conductivity," *Entropy*, vol. 22, no. 2, pp. 200, 2020. DOI: [10.3390/e22020200](https://doi.org/10.3390/e22020200).
- [50] J. Kierzenka and L. F. Shampine, "A BVP solver that controls residual and error," *J. Numer. Anal. Ind. Appl. Math.*, vol. 3, pp. 27–41, 2008.
- [51] A. Gilat and V. Subramaniam, *Numerical Methods for Engineers and Scientists: An Introduction with Applications Using MATLAB*. New York: Wiley, 2014.